Dissociative Electron Attachment to Di-*tert*-butylperoxide, Artemisinin, and *β*-Artemether

Alberto Modelli*

Dipartimento di Chimica "G. Ciamician", Università di Bologna, I-40126 Bologna, and Centro Interdipartimentale di Ricerca in Scienze Ambientali, Università di Bologna, I-48100 Ravenna, Italy

Vinicio Galasso

Dipartimento di Scienze Chimiche, Università di Trieste, I-34127 Trieste, Italy

Received: March 27, 2007; In Final Form: June 7, 2007

The gas-phase dissociative electron attachment spectra of di-*tert*-butylperoxide (DBP) and the antimalarial polycyclic peroxides artemisinin and *β*-artemether are presented for the first time. The total anion currents measured at the walls of the collision chamber and the mass selected anion currents are reported in the 0−6 eV energy range. Electron attachment to DBP produces an intense current, peaking at 1.3 eV, due to the $C_4H_9O^-$ negative fragment, in line with the strongly O−O antibonding character of the singly occupied orbital of the parent molecular anion and the small (if any) thermodynamic energy threshold predicted by B3LYP calculations for the formation of this anion fragment. A five times less intense signal, with $m/e = 57$ and a maximum at 0.7 eV, is also observed. The calculations exclude that this signal can be associated with the $C_4H_9^-$ negative fragment, whereas they support its assignment to the $C_3H_5O^-$ species, generated by simultaneous dissociation and loss of a methane molecule from the parent molecular anion. In DBP, artemisinin, and *β*-artemether, currents corresponding to the parent molecular anion are not detected, indicating that its survival time is shorter than the time required (about 10^{-6} s) to pass through the mass filter. In the latter two compounds, where simple O−O bond breaking does not generate separate fragments, the anion currents are much weaker than in DBP and the maximum total anion current peaks at zero energy.

Introduction

Artemisinin or qinghaosu (**1**) and its derivatives, sesquiterpenes containing a 1,2,4-trioxane ring and a highly reactive endoperoxidic bond, are a class of compounds widely used as antimalarial drugs, being effective against multi-drug-resistant malarial parasite strains such as *Plasmodium falciparum*.[1] In addition, it has recently been proven that artemisinin has antitumoral activity.[2] Although the mechanism of action has not yet been completely unveiled, the presence of the trioxane ring seems to be an essential feature to the pharmacological activity, with the peroxide group playing a key role in the first step.[3−6] A plausible conjecture is that in the biological medium Fe^{II} or Fe^{III} complexes (such as iron−porphyrin) can trigger the reaction mechanism, i.e., a reductive cleavage of the peroxide bond with production of local oxygen-centered radicals. These can in turn decay into more stable carbon-centered radicals, resulting in a cascade of reactions finally leading to the demise of the parasite.[7]

Over the past few years this subject has stimulated several studies, including nuclear magnetic resonance (NMR)[7] and electron spin resonance (ESR)[8−11] experiments. Theoretical calculations[12−14] have also been performed to characterize the energetics of the radical species produced by the iron heme and plausible reaction pathways. We have recently reported[15] a multidisciplinary theoretical and experimental study of artemisinin and selected derivatives to determine equilibrium geometries, normal vibrational modes, NMR chemical shifts, and gas-phase electronic structures. In particular, the vertical

electron attachment energies (VAEs) were measured[15] by means of electron transmission spectroscopy (ETS),[16] one of the most suitable means for detecting the formation of unstable anion states. Electron attachment to the lowest unoccupied molecular orbital (LUMO) of artemisinin, an antibonding σ^* MO essentially localized on the O−O bond, occurred around 1.7 eV. Although in the condensed phase all anion states are stabilized by the medium, the process of temporary electron capture (producing a shape resonance) in the gas phase is obviously correlated with chemical reduction in solution.

Additional information on temporary negative ion states is supplied by dissociative electron attachment spectroscopy (DEAS),[17] which measures the yield of negative fragments and long-lived molecular anions, as a function of the incident electron energy. When suitable energetic conditions occur, the decay of unstable molecular anions can follow a dissociative channel which generates negative fragments and neutral radicals

$$e^-_{(E)} + AX \rightarrow AX^{-*} \rightarrow A + X^-$$

in kinetic competition with simple re-emission of the extra electron. The lifetime of the negative fragments produced is usually sufficiently long to allow their detection by means of a mass filter. Measurements of the negative ion abundance, as a function of the incident electron energy, give insight into the nature and efficiency of the dissociative channels of resonance processes.

A recent study[18] has reported the DEA spectra of HOOH, but to our knowledge DEA studies of hydrocarbons containing a peroxide bond have not appeared in the literature. Here, we apply the DEAS technique to artemisinin (**1**, Scheme 1) and its

* Corresponding author. E-mail: alberto.modelli@unibo.it.

SCHEME 1:   Structural Formulas of Artemisinin (1),
β-Artemether (2), and Di-*tert*-butylperoxide (DBP)

DBP   1   2
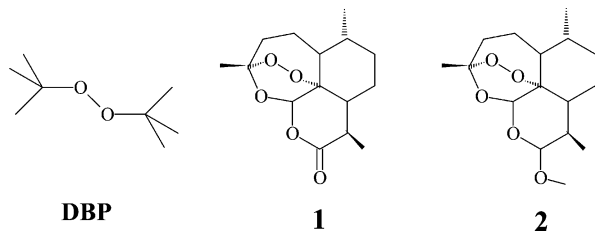
saturated derivative β-artemether (**2**) in the 0−6 eV energy range. Given that dissociation of a C−O or O−O bond in these polycyclic systems does not lead to formation of two separate fragments, the smaller reference molecule di-*tert*-butyl peroxide (DBP) is also analyzed. The results are interpreted with the support of density functional theory (DFT) calculations.

Experimental and Computational Details

The collision chamber of our ETS/DEAS apparatus[19] allows for ion extraction at 90° with respect to the electron beam direction. Negative ions are then accelerated and focused toward the entrance of a quadrupole mass filter. Alternatively, the total anion current can be collected and measured with a picoammeter at the walls of the collision chamber (about 0.8 cm from the electron beam). Measurements of the anion currents were obtained with an electron beam current of about 2×10^{-8} A. The electron beam resolution, obtained with a trochoidal monochromator, was about 100 meV (full width at half-maximum (fwhm)), as evaluated from the width of the SF_6^- signal at zero energy used for calibration of the energy scales. The estimated accuracy of the measured peak energies is ±0.1 eV. For artemisinin and β-artemether the sample inlet temperature required to generate sufficient vapor pressure was about 65 °C.

Calculations were performed with the Gaussian 03 set of programs.[20] The total energies of the neutral and anion states were obtained at the DFT level using the B3LYP hybrid functional,[21] with the standard 6-31G(d) and 6-31+G(d) basis sets, using the unrestricted formalism for the open-shell species.

The O−O and C−O gas-phase bond dissociation enthalpies were calculated using the MLM2 method, as recently suggested by Wright et al.[22] This procedure is defined in terms of energy// (geometry,frequency) as (RO)B3LYP/6-311+G(2d,2p)//B3LYP/ 6-31G(d); for the radical, the standard unrestricted method is used for geometry and frequency, but the restricted open-shell (RO) approach is used to calculate the final electronic energy. The electronic energies and the standard thermal corrections were then added to obtain the bond dissociation enthalpies that may be related to experimental values of $\Delta H°_{298}$.

Artemisinin and β-artemether were supplied by Alchem International (New Dehli, India).

Results and Discussion

Bond Dissociation Enthalpies. Before starting the discussion, a preliminary comment on the bond dissociation enthalpies is in order. According to the present MLM2 calculations, the bond dissociation enthalpy ($\Delta H°_{298}$) for the homolytic cleavage of the O−O bond in the gas phase is 37.6 kcal mol^{-1} (1.63 eV) for DBP, 30.2 (1.31 eV) kcal mol^{-1} for **1**, and 28.5 kcal mol^{-1} (1.24 eV) for **2**. It is satisfying to remark that the $\Delta H°_{298}$ calculated for DBP is in fair agreement with available experimental values,[23−26] which range from 38.0 to 42.9 kcal mol^{-1}. On the other hand, the O−O $\Delta H°_{298}$ calculated for the strained
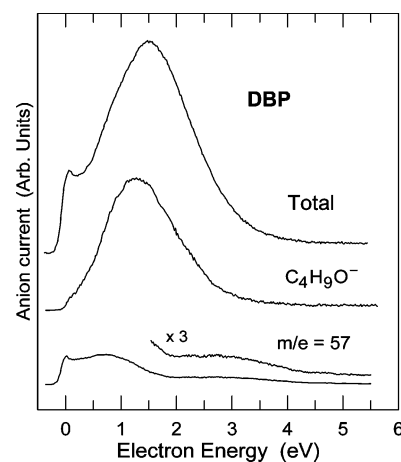
Figure 1. Total and fragment anion currents, as a function of the incident electron energy, measured for DBP.

TABLE 1: Peak Energies (eV) Measured in the Total and the Fragment Anion Currents Observed through a Mass Filter and Relative Intensities (from Peak Heights) of the Fragment Anion Currents

	total current peak energy	fragment anion current		
		peak energy	*m/e*	rel intens (%)
di-*tert*-butylperoxide		2.6	57	5
(DBP)	1.5	1.3	73	100
		0.7	57	19
	0.0	0.0	57	18
artemisinin (**1**)	1.1	1.1	184	3
		0.7	45	7
	0.0	0.0	45, 184, 254	100, 5, 13
β-artemether (**2**)	1.6	1.9	168	very weak
	0.0			

endoperoxides **1** and **2** is smaller by ca. 7−9 kcal mol^{-1} relative to that of the acyclic peroxide DBP (where cleavage leads to two radical fragments), consistent with the estimate based on careful electrochemical methods by Workentin and Donkers.[27,28] Furthermore, the acetal derivation of **1** to give **2** results in a slight decrease of the O−O $\Delta H°_{298}$. As to the C−O $\Delta H°_{298}$, the MLM2 calculations for DBP yield a value of 79.9 kcal mol^{-1} (3.46 eV), similar to the experimental value of 83.0 kcal mol^{-1} determined for $H_3C−OC_2H_5$.[29]

Because the biological activity of artemisinin drug molecules occurs in solution, it was considered useful to gain some information on the O−O $\Delta H°_{298}$ in a solvated environment, namely, aqueous solution, using MLM2 and the continuum polarization model (PCM).[30] In particular, full solution-phase calculations were carried out for DBP, whereas the gas-phase results were combined with (RO)B3LYP/6-311+G(2d,2p) single-point energies for **1** and **2**. According to these calculations, solvation causes a slight decrease (ca. 1−3 kcal mol^{-1}) of the O−O $\Delta H°_{298}$, the aqueous-phase values being 37.6 (DBP), 29.1 (**1**), and 27.3 kcal mol^{-1} (**2**).

It may be anticipated that the pattern of these theoretical results is consistent with the conclusions based on the DEAS results, as discussed in the following paragraphs.

DEAS Results. The upper curve of Figure 1 reports the total anion current measured for DBP at the walls of the collision chamber, as a function of the incident electron energy, over the 0−6 eV energy range. The total anion current displays a sharp rise at zero energy and an intense and broad (about 1.8 eV fwhm) signal peaking at 1.5 eV. Consistently, the ET spectrum of DBP[15] shows a broad resonance centered at 2.0 eV, ascribed to electron capture into the σ* LUMO, mainly localized on the

DEAS of Peroxides

J. Phys. Chem. A, Vol. 111, No. 32, 2007 **7789**
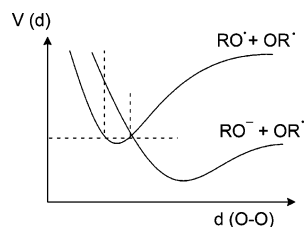
Figure 2. Schematic representation of the potential energy curves of a peroxide (ROOR) and its anion, as a function of O−O distance.
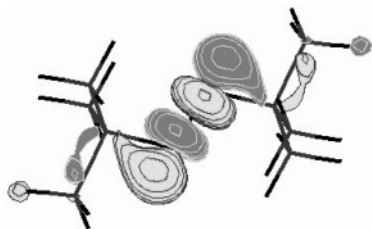
Figure 3. Representation of the LUMO of DBP, as supplied by B3LYP/6-31G(d) calculations.

TABLE 2: B3LYP/6-31G(d) Empty MO Energies of DBP

orbital	energy (eV)	orbital	energy (eV)
σ^*_{COOC}	3.596	σ^*_{CH}	2.239
σ^*_{CO}	3.225	σ^*_{OO}	0.875
σ^*_{CH}	2.874		

O−O bond. Although contributions from higher lying empty MOs to the resonance observed in ETS cannot be excluded, B3LYP/6-31G(d) calculations (see Table 2) predict the energy gap between the LUMO and second LUMO to be rather large.

The shift of the peaks to lower energy in the DEA spectra with respect to the corresponding resonances observed in ETS is well-understood in terms of shorter lifetime and greater distance to the crossing between the anion and neutral potential curves for the anions formed on the high-energy side of the resonance[31] (see scheme in Figure 2). This shift can be quite large (for instance, about 1 eV in 1-chloroalkanes[32]), depending in an inverse fashion upon the resonance lifetime.

Due to the strongly O−O antibonding character of the LUMO of DBP (Figure 3), the predominant dissociation decay channel of the parent molecular anion is expected to involve cleavage of the peroxide bond. In agreement, the most abundant negative fragment found in HOOH is OH⁻, the HO_2^- current (if any) being barely measurable.[18] In line with this expectation, the mass selected DEA spectra of DBP (see Figure 1 and Table 1) display an intense negative current with $m/e = 73$, corresponding to the negative fragment $C_4H_9O^-$ generated by cleavage of the O−O bond in the parent molecular anion.

A current with $m/e = 57$ is also observed, although five times less intense than that with $m/e = 73$. Moreover, while the latter peaks at 1.3 eV, the $m/e = 57$ signal has a maximum at only 0.7 eV. The $m/e = 57$ cross-section also displays a smaller maximum at about 2.6 eV, reasonably associated with dissociation of a higher lying shape resonance or core-excited resonance, i.e., simultaneous electron addition and excitation of the neutral state.

Signals due to the DBP⁻ parent molecular anion ($m/e = 146$) were not detected, thus indicating that its lifetime is short relative to the time (of the order of 1 μs) requested to pass through the mass filter. Currents with $m/e = 89$ or 32 (associated with the $C_4H_9OO^-$ and O_2^- negative species, respectively) were not detected.

The B3LYP results (including only electronic contributions) for the energetics of dissociative processes of the DBP anion

TABLE 3: B3LYP Energies (Only Electronic Contributions, eV) Relative to the Neutral State of DBP

		6-31G(d)	6-31+G(d)	
1	$t\text{-}C_4H_9OOt\text{-}C_4H_9$	0	0	
2	$t\text{-}C_4H_9OOt\text{-}C_4H_9^-$ (vertical anion)	2.931	1.163 ^{a}	(vertical AE)
3	$t\text{-}C_4H_9OOt\text{-}C_4H_9^-$ (adiabatic anion)	-0.632	−1.178	(adiabatic AE)
4	$t\text{-}C_4H_9O^\bullet + t\text{-}C_4H_9O^\bullet$	1.526	1.325	(O−O BDE)
5	$t\text{-}C_4H_9^\bullet + t\text{-}C_4H_9OO^\bullet$	2.645	2.533	(C−O BDE)
6	$t\text{-}C_4H_9O^\bullet + t\text{-}C_4H_9O^-$	0.626	−0.399	
7	$t\text{-}C_4H_9^\bullet + t\text{-}C_4H_9OO^-$	2.425	1.532	
8	$t\text{-}C_4H_9^- + t\text{-}C_4H_9OO^\bullet$	3.749	2.793	
9	$t\text{-}C_4H_9^\bullet + O_2 + t\text{-}C_4H_9^-$	5.228	4.256	
10	$t\text{-}C_4H_9O^\bullet + CH_4 + C_3H_5O^-$	0.409	−0.611	

^{a} The SOMO is described as a diffuse function.

are given in Table 3. It is worth noting that a theoretical approach adequate for describing the energetics and nature of anion states involves difficulties not encountered for neutral or cation states. A proper description of the spatially spread electron distributions of anions requires a basis set with diffuse functions.[33] On the other hand, inclusion of diffuse functions can generate low-energy solutions with no physical significance for anion formation,[34−37] mainly for anion states which are unstable with respect to the neutral molecule.

As expected,[36,37] the 6-31G(d) basis set, which does not include diffuse functions, overestimates the anion energies. In fact, the total energy (relative to the neutral state) of the vertical molecular anion (i.e., with the same geometry of the optimized neutral state) is calculated to be 2.9 eV (second row of Table 3), to be compared with a sizably smaller VAE (2.0 eV) measured in the ET spectrum.[15] However, even the smallest addition of diffuse functions (6-31+G(d) basis set) causes the LUMO of the neutral state and the singly occupied MO (SOMO) of the vertical parent molecular anion of DBP to be described as a spatially diffuse σ^* MO rather than a valence σ^*_{OO} MO, so that comparison of the 6-31+G(d) VAE (1.2 eV) with experiment is irrelevant. The optimized anion is also predicted to be more stable than the neutral state with the 6-31G(d) basis set, namely, with a positive adiabatic electron affinity (plausibly underestimated) of 0.6 eV (1.2 eV with the 6-31+G(d) basis set, and in this case the SOMO is not a diffuse function).

The SOMOs of the neutral radicals $t\text{-}C_4H_9{}_\bullet$, $t\text{-}C_4H_9O^\bullet$, and $t\text{-}C_4H_9OO^\bullet$, as well as the HOMOs of the negative fragments $t\text{-}C_4H_9^-$, $t\text{-}C_4H_9O^-$, $t\text{-}C_4H_9OO^-$, and $C_3H_5O^-$, are correctly described as valence MOs even with the 6-31+G(d) basis set. The O−O and C−O bond dissociation energies (BDEs, only electronic contributions) of the neutral molecule are given in rows 4 and 5 of Table 3. The C−O BDE is calculated to be sizably larger (>1 eV) than the O−O BDE with both basis sets 6-31G(d) and 6-31+G(d), in full agreement with the corresponding aforementioned $\Delta H°_{298}$.

The thermodynamic threshold for production of the negative fragments is likely overestimated by the 6-31G(d) basis set (as expected when negative ions are involved). A threshold of 0.6 eV is predicted for production of the $t\text{-}C_4H_9O^-$ and $t\text{-}C_4H_9O^\bullet$ fragments (see row 6 of Table 3), whereas the 6-31+G(d) calculations predict the absence of an energy threshold, the two fragments being more stable than the neutral molecule.

In contrast, the energy threshold for breaking the C−O bond of the parent anion to produce the $t\text{-}C_4H_9OO^-$ and $t\text{-}C_4H_9^\bullet$ fragments is calculated to be fairly large (1.5 eV with the 6-31+G(d) calculations, row 7 of Table 3). Because of the smaller electron affinity of the $t\text{-}C_4H_9^\bullet$ neutral radical with

7790 *J. Phys. Chem. A, Vol. 111, No. 32, 2007*

Modelli and Galasso
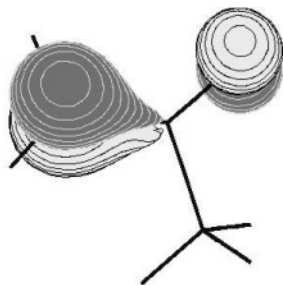
Figure 4. Representation of the HOMO of $C_3H_5O^-$, as supplied by B3LYP/6-31G(d) calculations.

respect to $t\text{-}C_4H_9OO^{\bullet}$, the calculated energy threshold to produce the $t\text{-}C_4H_9OO^{\bullet}$ and $t\text{-}C_4H_9^-$ fragments is even larger (Table 3, row 8).

The above results, together with the calculated localization properties of the LUMO of DBP, clearly indicate that dissociation of the O−O bond of the parent molecular anion is by far favored with respect to that of the C−O bond, in agreement with experiment. The absence of $C_4H_9OO^-$ negative currents even at energies higher than the thermodynamic threshold can be explained in terms of kinetic factors; i.e., the time required for dissociation to occur along the C−O bond is long compared with the survival time (with respect to re-emission of the added electron) of (first or excited) parent anion states formed above the thermodynamic threshold.

Turning now to the $m/e = 57$ anion current displayed in Figure 1, the mass of this negative fragment coincides with that of the butyl group, one of the two fragments produced by simple cleavage of a C−O bond in the parent molecular anion. However, as obvious as the assignment of the $m/e = 57$ signal to $t\text{-}C_4H_9^-$ might seem, the calculated energy threshold (2.8 eV with the 6-31+G(d) basis set) for its production, together with the experimentally verified absence of the $C_4H_9OO^-$ fragment (thermodynamically favored in the case of C−O bond breaking, see Table 3), convincingly rules out the hypothesis of dissociation of the C−O bond to generate a $t\text{-}C_4H_9^-$ current with maxima at thermal electron energies and 0.7 eV, as found experimentally.

To further explore the possibility that the $m/e = 57$ current is due to the $C_4H_9^-$ anion, we have conjectured the occurrence of a process more complex than simple C−O cleavage, i.e., rearrangement of the parent molecular anion and multiple dissociation to give the two neutral species O_2 and $t\text{-}C_4H_9^{\bullet}$, and the $t\text{-}C_4H_9^-$ anion. According to the calculations, however, the energy threshold for this process is sizably higher (about 1.5 eV, compare rows 9 and 8 of Table 3) than that for direct production of $t\text{-}C_4H_9^-$ from C−O cleavage.

Interestingly, however, the $m/e = 57$ negative current can be associated with the $C_3H_5O^-$ negative fragment instead of the butyl anion. This species can be generated by cleavage of the O−O bond and loss of a neutral methane molecule from the parent DBP$^-$ anion. According to the calculations (compare rows 10 and 6 of Table 3), the total energy of the three species $t\text{-}C_4H_9O^{\bullet}$, CH_4, and $C_3H_5O^-$ is 0.2 eV smaller than that of the $t\text{-}C_4H_9O^{\bullet}$ and $t\text{-}C_4H_9O^-$ species. The $C_3H_5O^-$ anion possesses a three-center π-system. A representation of its HOMO, as supplied by B3LYP/6-31G(d) calculations (quite similar to that obtained with the 6-31+G(d) basis set) is given in Figure 4, and the calculated H_2C-C and C−O bond distances are 1.384 and 1.272 Å, respectively.

In principle, the $C_3H_5O^-$ anion could be formed by quick loss of CH_4 from the $t\text{-}C_4H_9O^-$ fragment anion. In this case, however, one would expect the $m/e = 57$ and 73 DEA cross-
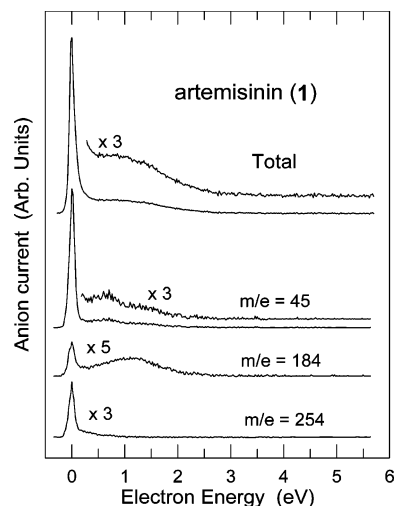
Figure 5. Total and fragment anion currents, as a function of incident electron energy, measured in artemisinin (**1**).

sections to resemble each other in shape (in contrast with experiment), unless the $t\text{-}C_4H_9O^-$ fragments which lose methane were formed from a different starting parent anion state. The latter hypothesis, however, is not supported by the calculations, according to which the second and third LUMO of DBP are mainly localized on the C−H bonds and lie at sizably higher energy than the LUMO (see Table 2). More plausibly, the first anion state of DBP (in addition to simple dissociation of the O−O bond) can follow a more complex decay channel through concerted nuclear rearrangement, O−O dissociation, and CH_4 loss:

$$DBP^- \rightarrow t\text{-}C_4H_9O^{\bullet} + CH_4 + C_3H_5O^-$$
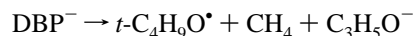
The complexity of this path likely requires a relatively long survival time of the parent molecular anion, thus accounting for both the smaller cross-section of the $m/e = 57$ current and the occurrence of its maximum at only 0.7 eV (due to the inverse dependence of lifetime on energy). Measurements on isotopically substituted DBP could supply further evidence for the presence of the oxygen atom in the $m/e = 57$ negative fragment.

Finally, although the difference is close to the estimated errors, the maximum of the total anion current seems to be located at 0.2 eV higher energy than the peak of the most intense ($C_4H_9O^-$) fragment current. This suggests that the survival time of the parent molecular anion could be sufficiently long to give some contribution to the total anion current (measured at only 0.8 cm from the incident electron beam).

Figure 5 reports the DEA spectra of artemisinin. The total anion current displays a sharp and intense peak at zero energy, followed by a weak and broad feature centered at about 1.1 eV. The corresponding shape resonance observed in the ET spectrum[15] is located at 1.76 eV and has been ascribed to the unresolved contributions from electron capture into the first two (with mainly σ^*_{OO} and carbonyl π^*_{CO} character, respectively) empty MOs. At variance with DBP, the largest dissociative cross-section of **1** occurs at zero energy, where the inverse energy dependence of the electron attachment cross-section for the s wave causes the yield to climb.[38] In fact, in contrast with DBP, here simple breaking of the corresponding O−O (or C−O) bond does not lead to formation of anion fragments.

The mass-selected DEA spectra of **1** (see Figure 5 and Table 1) show negative fragment currents at $m/e = 45$, 184, and 254. The $m/e = 45$ and 254 signals can plausibly be associated with the COOH$^-$ and (M−CO)$^-$ fragments (where M = parent

DEAS of Peroxides

J. Phys. Chem. A, Vol. 111, No. 32, 2007 **7791**
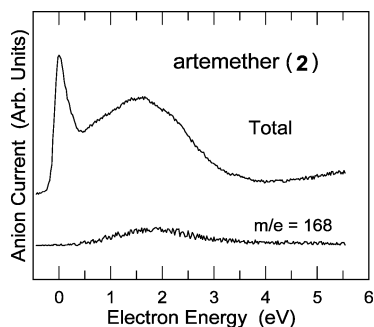
Figure 6. Total and fragment anion currents, as a function of incident electron energy, measured in β-artemether (**2**).

Figure 7. Representation of the SOMO of the geometrically relaxed anion of artemisinin, as supplied by B3LYP/6-31G(d) calculations.
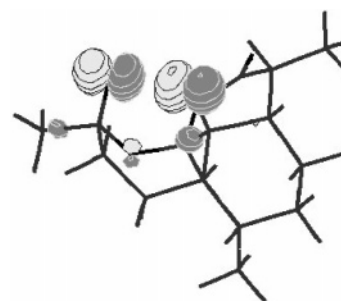
molecular anion), respectively. To conjecture which fragment is associated with the $m/e = 184$ signal is less straightforward. This current is the weakest of the three, but the only one which displays a distinct maximum at 1.1 eV, thus paralleling the total anion current. In any case, all three fragments stem from multiple bond cleavage and probably also involve rearrangement processes, in line with the weakness of these signals relative to the t-$C_4H_9O^-$ current in DBT.

The DEA spectra of the saturated derivative β-artemether are displayed in Figure 6. The total anion current presents some differences with respect to **1**. In **2**, the zero energy peak is followed by a broad signal of comparable height. Its maximum occurs at an energy (1.6 eV) close to that (1.7 eV) of the center of the resonance observed in ETS.[15] Analysis through the mass filter revealed only a very weak signal at $m/e = 168$, consistent with CO loss from the parent molecular anion ($m/e = 296$). The energy of its maximum (about 1.9 eV) suggests that this negative fragment is not generated by dissociation of the first anion state.

As found in DBP, also in **1** and **2** no signals due to the parent molecular anion ($m/e = 282$ and 296, respectively) were detected in the mass-selected spectra. However, the parent molecular anion likely gives a significant contribution to the total negative current measured at the walls of the collision chamber, mainly in **2** where the fragment negative current is very weak and cannot account for the observed total anion current.

Table 4 reports the B3LYP/6-31G(d) energies (relative to the neutral molecule) of the vertical and adiabatic anions of DBP, **1**, and **2**, together with calculated bond distances for the optimized neutral and anion states. The geometrical parameters obtained with the 6-31+G(d) basis set (reported in parentheses) are only slightly larger than those obtained with the smaller basis set. The available experimental O–O bond distance of DBP (1.478 Å [39]) is accurately reproduced.

The B3LYP/6-31G(d) VAE of **1**, at variance with DBP and **2**, is quite close to the experimental value (1.76 eV [15]). This is

probably due to the fact that, in contrast with the LUMO of the neutral molecule and the SOMO of the adiabatic anion (which essentially possess only σ^*_{OO} character), the calculations predict the SOMO of the vertical anion of **1** to bear also a significant π^*_{CO} character.

On going from the neutral molecules **1** and **2** to their geometrically relaxed anions (see Table 4), the O–O bond distance increases from about 1.5 to 2.2 Å, whereas the adjacent C–O bond distances shorten by about 0.1 Å. Even at this large separation between the oxygen atoms, the SOMO of the adiabatic anion state is still described as an antibonding σ^*_{OO} MO, as represented in Figure 7 for artemisinin. While in the gas phase the vertical anion formed by resonance cannot dissipate energy, in the condensed phase the molecular anion can lose energy by collisions with the solvent (which also stabilizes all negative species) and reach its optimized geometry. It is thus probably this species, where the peroxide bond is lengthened, that gives rise to the chain of rearrangements and reactions which lead to the antimalarial activity.

Concluding Remarks

The dissociative decay channels of the gas-phase temporary molecular anions of compounds containing a peroxide bond have been investigated. Dissociative electron attachment spectroscopy, by measuring both the total anion current (at 0.8 cm from the incident electron beam) and the anion currents selected through a mass filter, has been applied to the polycyclic sesquiterpenes artemisinin and β-artemether and the smaller reference molecule di-$tert$-butyl peroxide (DBP). The first two compounds are widely used as antimalarial drugs. The first step of the mechanism of their activity consists of a reductive cleavage of the peroxide bond, thus paralleling the gas-phase temporary electron capture process occurring in the present experiment.

The mass selected DEA spectra of DBP show production of negative fragments with $m/e = 73$ and 57. The former intense signal (associated with $C_4H_9O^-$) peaks at 1.3 eV and comes from dissociation of the O–O bond of the parent molecular

TABLE 4: B3LYP/6-31G(d) Energies (Only Electronic Contributions) Relative to the Neutral Molecules and Bond Distances (Å)[a]

	energy (eV)	d_{O-O}	d_{C-O}	d'_{C-O}	$d_{C=O}$
DBP	0	1.474 (1.475)	1.442 (1.446)		
DBP⁻ (vertical anion)	2.931 (VAE)				
DBP⁻ (adiabatic anion)	−0.632	2.37 (2.387)	1.375 (1.381)		
artemisinin	0	1.460 (1.460)	1.455 (1.458)	1.414 (1.416)	1.207 (1.210)
artemisinin⁻ (vertical anion)	1.917 (VAE)				
artemisinin⁻ (adiabatic anion)	−1.438	2.185 (2.199)	1.370 (1.375)	1.325 (1.331)	1.220 (1.223)
β-artemether	0	1.462 (1.462)	1.460 (1.461)	1.412 (1.415)	
β-artemether⁻ (vertical anion)	2.521 (VAE)				
β-artemether⁻ (adiabatic anion)	−1.057	2.214 (2.230)	1.371 (1.377)	1.324 (1.330)	

[a] The geometrical parameters reported in parentheses are obtained with the 6-31+G(d) basis set.

anion, in line with the strongly O−O antibonding character of the σ^* LUMO of DBP and the fact that cleavage of the peroxide bond is largely thermodynamically favored with respect to the C−O bond (as predicted by B3LYP calculations). Although assignment of the $m/e = 57$ signal (which displays maxima at zero and 0.7 eV) to the t-$C_4H_9^-$ fragment would seem straightforward, according to the calculations cleavage of the C−O bond of the parent molecular anion cannot occur at this energy, even in the case of formation of the energetically more favored t-$C_4H_9OO^-$ negative species (which is in fact not detected). The $m/e = 57$ current can be explained by the occurrence of a more complex decay channel (nuclear rearrangement and multiple bond dissociation) of the DBP$^-$ parent anion, with production of the t-$C_4H_9O\bullet$ neutral radical, a CH_4 neutral molecule, and the $C_3H_5O^-$ anion. The energy of the two latter species is in fact calculated to be smaller than that of the t-$C_4H_9O^-$ anion. Future measurements on isotopically substituted DBP could supply further evidence for the presence of the oxygen atom in the $m/e = 57$ negative fragment.

In the polycyclic peroxides artemisinin and β-artemether (as well as in DBP), the lifetime of the parent molecular anion is not sufficiently long to allow its detection through the mass filter. In addition, simple O−O bond breaking cannot lead to formation of two separate fragments. In agreement, only weak fragment anion currents are observed, associated with multiple bond cleavage and rearrangement processes. The maximum total anion current, measured close to the incident electron beam, occurs at zero energy and likely has a significant contribution from the parent molecular anion.

According to B3LYP calculations, in the geometrically relaxed (adiabatic) parent anions of artemisinin and β-artemether, the added electron is mainly localized (in an antibonding manner) on the peroxidic oxygen atoms, although their distance increases to about 2.2 Å.

References and Notes

(1) World Health Organization. *Trans. R. Soc. Trop. Med. Hyg.* **2000**, *94* (Suppl. 1), 36.

(2) Meschnick, S. R.; Taylor, T. E.; Kamchonwongpaisan, S. *Microbiol. Rev.* **1996**, *60*, 301.

(3) Brossi, A.; Venugopalan, B.; Gerpe, L. D.; Yeh, H. J.; Flippen-Anderson, J. L.; Buchs, P.; Luo, X. D.; Milhous, W.; Peters, W. *J. Med. Chem.* **1988**, *31*, 645.

(4) Cumming, J. N.; Ploypradith, P.; Posner, G. *Adv. Pharmacol.* **1996**, *37*, 253.

(5) Jefford, C. W.; Vicente, M. G. H.; Jacquier, Y.; Favarger, F.; Mareda, J.; Millasson-Schmidt, P.; Brunner, G.; Burger, U. *Helv. Chim. Acta* **1996**, *79*, 1475.

(6) Meshnick, S. R. *Int. J. Parasitol.* **2002**, *32*, 1655.

(7) Posner, G. H.; Oh, C. H. *J. Am. Chem. Soc.* **1992**, *114*, 8328.

(8) Robert, A.; Boularan, M.; Meunier, B. *C. R. Acad. Sci., Ser. IIa: Sci. Terre Planets* **1997**, *324*, 59.

(9) Wu, W.-M.; Wu, Y.; Wu, Y.-L.;. Yao, Z.-J.; Zhou, C.-M.; Li, Y.; Shan, F. *J. Am. Chem. Soc.* **1998**, *120*, 3316.

(10) O'Neill, P. M.; Miller, A.; Bishop, L. P. D.; Hindley, S.; Maggs, J. L.; Ward, S. A.; Roberts, S. M.; Scheinmann, F.; Stachulski, A. V.; Posner, G. H.; Park, B. K. *J. Med. Chem.* **2001**, *44*, 58.

(11) Alberti, A.; Macciantelli, D.; Marconi, G. *Res. Chem. Intermed.* **2004**, *30*, 615.

(12) Gu, J.; Chen, K.; Jiang, H.; Leszczynski, J. *J. Mol. Struct. (THEOCHEM)* **1999**, *491*, 57.

(13) Tonmunphean, S.; Parasuk, V.; Kokpol, S. *J. Mol. Struct. (THEOCHEM)* **2005**, *724*, 99.

(14) Tonmunphean, S.; Parasuk, V.; Kokpol, S. *Bioorg. Med. Chem.* **2006**, *14*, 2082.

(15) Galasso, V.; Kovač, B.; Modelli, A. *Chem. Phys.* **2007**, *335*, 141.

(16) Sanche, L.; Schulz, G. *Phys. Rev. A* **1972**, *5*, 1672.

(17) Schulz, G. J. *Rev. Mod. Phys.* **1973**, *45*, 378, 423.

(18) Nandi, D.; Krishnakumar, E.; Rosa, A.; Schmidt, W.-F.; Illenberger, E. *Chem. Phys. Lett.* **2003**, *373*, 454.

(19) Modelli, A.; Foffani, A.; Scagnolari, F.; Jones, D. *Chem. Phys. Lett.* **1989**, *163*, 269.

(20) Frisch, M. J.; Trucks, G. W.; Schlegel, H. B.; Scuseria, G. E.; Robb, M. A.; Cheeseman, J. R.; Zakrzewski, V. G.; Montgomery, J. A., Jr.; Stratmann, R. E.; Burant, J. C.; Dapprich, S.; Millam, J. M.; Daniels, A. D.; Kudin, K. N.; Strain, M. C.; Farkas, O.; Tomasi, J.; Barone, V.; Cossi, M.; Cammi, R.; Mennucci, B.; Pomelli, C.; Adamo, C.; Clifford, S.; Ochterski, J.; Petersson, G. A.; Ayala, P. Y.; Cui, Q.; Morokuma, K.; Malick, D. K.; Rabuck, A. D.; Raghavachari, K.; Foresman, J. B.; Cioslowski, J.; Ortiz, J. V.; Stefanov, B. B.; Liu, G.; Liashenko, A.; Piskorz, P.; Komaromi, I.; Gomperts, R.; Martin, R. L.; Fox, D. J.; Keith, T.; Al-Laham, M. A.; Peng, C. Y.; Nanayakkara, A.; Gonzalez, C.; Challacombe, M.; Gill, P. M. W.; Johnson, B.; Chen, W.; Wong, M. W.; Andres, J. L.; Gonzalez, C.; Head-Gordon, M. E.; Replogle, S.; Pople, J. A. *Gaussian 03*, Revision B.05; Gaussian Inc.: Pittsburgh, PA, 2003.

(21) Becke, A. D. *J. Chem. Phys.* **1993**, *98*, 5648.

(22) Wright, J. S.; Rowley, C. N.; Chepelev, L. L. *Mol. Phys.* **2005**, *103*, 815.

(23) McMillen, D. F.; Golden, D. M. *Annu. Rev. Phys. Chem.* **1982**, *33*, 493.

(24) Reints, W.; Pratt, D. A.; Korth, H.-G.; Mulder, P. *J. Phys. Chem. A* **2000**, *104*, 10713.

(25) Borges do Santos, R. M.; Muralha, V. S. F.; Correia, C. F.; Martinho Simões, J. A. *J. Am. Chem. Soc.* **2001**, *123*, 12670.

(26) DeTuri, V. F.; Ervin, K. M. *J. Phys. Chem. A* **1999**, *103*, 6911.

(27) Workentin, M. S.; Donkers, R. L. *J. Am. Chem. Soc.* **1998**, *120*, 2664.

(28) Donkers, R. L.; Workentin, M. S. *J. Phys. Chem. B* **1998**, *102*, 4061.

(29) DiLabio, G. A.; Pratt, D. A. *J. Phys. Chem. A* **2000**, *104*, 1938.

(30) Barone, V.; Cossi, M.; Tomasi, J. *J. Chem. Phys.* **1997**, *107*, 3210.

(31) O'Malley, T. F. *Phys. Rev.* **1966**, *150*, 14.

(32) Guerra, M.; Jones, D.; Distefano, G.; Scagnolari, F.; Modelli, A. *J. Chem. Phys.* **1991**, *94*, 484.

(33) Dunning, T. H., Jr.; Peterson, K. A; Woon, D. E. Basis Sets: Correlation Consistent Sets. In *Encyclopedia of Computational Chemistry*; Schleyer, P. v. R., Ed.; Wiley: Chichester, U.K., 1998.

(34) Burrow, P. D.; Howard, A. E.; Johnston, A. R.; Jordan, K. D. *J. Phys. Chem.* **1992**, *96*, 7570.

(35) Staley, S. S.; Strnad, J. T. *J. Phys. Chem.* **1994**, *98*, 161.

(36) Modelli, A.; Hajgató, B.; Nixon, J. F.; Nyulászi, L. *J. Phys. Chem. A* **2004**, *108*, 7440.

(37) Modelli, A. *Phys. Chem. Chem. Phys.* **2003**, *5*, 2923.

(38) Chutjian, A.; Alajajian, S. H. *Phys. Rev. A* **1985**, *31*, 2885.

(39) Kosnikov A. Yu.; Antonovsky, V. L.; Lindeman, S. V.; Antipin, M. Yu.; Struchkov, Yu. T.; Turovskii, N. A.; Zyat'kov, I. P. *Teor. Eksp. Khim.* **1989**, *25*, 82.